IL NUOVO CIMENTO **39 C** (2016) 339
DOI 10.1393/ncc/i2016-16339-1

COLLOQUIA: La Thuile 2016

Top quark production measurements with CMS

A. JAFARI(*) on behalf of the CMS COLLABORATION
Université Catholique de Louvain - Louvain-la-Neuve, Belgium

received 26 July 2016

Summary. — An overview of the CMS top quark cross section measurements with the focus on the latest results is presented.

1. – Introduction

More than 20 years after its discovery, the top quark [1, 2] is still considered an effective testing ground to validate the standard model (SM) or to see hints for new physics connected to this heaviest known particle. At the CERN Large Hadron Collider (LHC) the top quark is predominantly produced through strong interactions in pair ($\mathrm{t\bar{t}}$) and to lesser extent in single mode via electroweak processes. The latter has three production mechanisms, t-channel, tW and s-channel, ordered by their rate at the LHC. The $\mathrm{t\bar{t}}$ and single-top cross sections have been measured by the CMS experiment [3] with an unprecedented precision using the LHC Run I data [4-6]. The large data sample of top quarks recorded by the CMS experiment is also exploited to validate Monte Carlo generators and theory calculations through inclusive and differential measurements of the top quark cross section and properties in the full phase space or within the detector acceptance. With the LHC start up in 2015, colliding protons at $\sqrt{s} = 13\,\mathrm{TeV}$, top quark events were used as a commissioning tool thanks to the diversity of particles in their final state, *i.e.*, $\mathrm{t} \to \mathrm{bW} \to \mathrm{b}\ell\nu$ and/or $\mathrm{t} \to \mathrm{bW} \to \mathrm{bqq'}$. The CMS experiment has performed inclusive and differential cross section measurements using the very first 13 TeV proton collisions and soon, updated the analyses with the entire 2015 data. The inclusive $\mathrm{t\bar{t}}$ cross sections are already limited by systematic uncertainties.

2. – Run I legacy $\sigma_{\mathrm{t\bar{t}}}$ measurement in the ℓ+jets and $e\mu$ final states

In the ℓ+jets analysis [7] events with exactly one isolated high p_{T} muon or electron, originating from the vertex of the interaction, are required to have at least four jets of

(*) E-mail: abideh.jafari@cern.ch

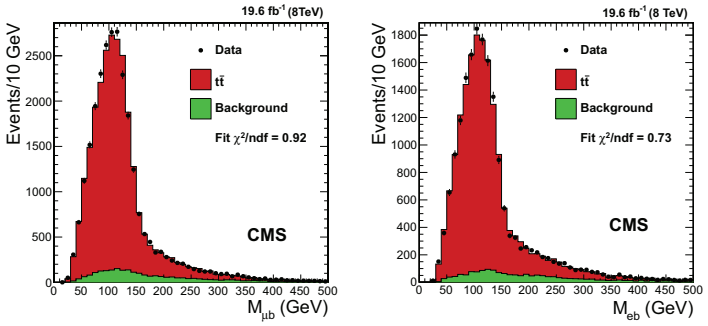

(a) (b)

Fig. 1. – Distributions of the lepton-jet mass in the muon+jets (a) and electron+jets (b) channels, rescaled to the fit results [7].

which one is likely to be coming from a b quark. The hadronically decaying top quark is reconstructed using the three jet combination minimizing a χ^2 value which is constrained by the mass of the top quark and the W boson. The energy of the jets assigned to the W boson are recalibrated using m_{W} constraint. The $M_{\ell b}$ variable is defined as the invariant mass of the selected lepton and the remaining jet which is supposedly a b-quark jet. It is used to extract the top quark cross section as well as the b-quark jet identification efficiency. Figure 1 illustrates the $M_{\ell b}$ distributions for the electron and muon channel of the analysis. To extract $\sigma_{\mathrm{t\bar{t}}}$, binned maximum likelihood fits to these distributions are performed and the results are combined using the BLUE method. The combined cross section is measured in the fiducial volume and extrapolated to the full phase space, yielding $\sigma_{\mathrm{t\bar{t}}}(8\,\mathrm{TeV}) = 228.5 \pm 3.8\,(\mathrm{stat.}) \pm 13.7\,(\mathrm{syst.}) \pm 6.0\,(\mathrm{lumi.})\,\mathrm{pb}$, compatible with SM predictions, $\sigma_{\mathrm{t\bar{t}}} = 252.89^{+13.3}_{-14.5}\,\mathrm{pb}$. The dominant systematic uncertainties are from Jet Energy Scale (JES) and signal modeling. The $\sigma_{\mathrm{t\bar{t}}}(7\,\mathrm{TeV})$ is measured with a similar method leading to a cross section ratio of $R_{\mathrm{t\bar{t}}} \equiv \frac{\sigma_{\mathrm{t\bar{t}}}(8\,\mathrm{TeV})}{\sigma_{\mathrm{t\bar{t}}}(7\,\mathrm{TeV})} = 1.43 \pm 0.09$, in agreement with the SM calculations, 1.43 ± 0.01. The analysis at 8 TeV (7 TeV) uses 19.7 (5.0) fb^{-1} of the LHC collision data.

A multidifferential measurement of $\sigma_{\mathrm{t\bar{t}}}$ is carried out [8] using events with exactly one electron and one muon in the final state. Events are classified according to the number of b-quark jets and number of additional jets that are not identified as b-jets. A simultaneous likelihood fit is performed, in all categories, to the p_{T} distribution of the softest jet, reducing the systematic uncertainties due to extra radiations in the event. The analysis uses the data at $\sqrt{s} = 7\,\mathrm{TeV}$ and $\sqrt{s} = 8\,\mathrm{TeV}$, corresponding to an integrated luminosity of 5.0 and $19.7\,\mathrm{fb}^{-1}$, respectively. The measurements result in $\sigma_{\mathrm{t\bar{t}}}(7\,\mathrm{TeV}) = 173.6 \pm 2.1\,(\mathrm{stat.})^{+4.5}_{-4.0}\,(\mathrm{syst.}) \pm 3.8\,(\mathrm{lumi.})\,\mathrm{pb}$ and $\sigma_{\mathrm{t\bar{t}}}(8\,\mathrm{TeV}) = 244.9 \pm 1.4\,(\mathrm{stat.})^{+6.3}_{-5.5}\,(\mathrm{syst.}) \pm 6.4\,(\mathrm{lumi.})\,\mathrm{pb}$, with a cross section ratio of $R_{\mathrm{t\bar{t}}} = 1.41 \pm 0.06$. All measurements are in agreement with the SM expectations. Figure 2 shows the post-fit p_{T} distribution of the least energetic jet in the event, in different categories at $\sqrt{s} = 7\,\mathrm{TeV}$.

3. – The $\sigma_{\mathrm{t\bar{t}}}$ measurement in the $e\mu$ final state at 13 TeV

The first $42\,\mathrm{pb}^{-1}$ of the LHC proton collisions at $\sqrt{s} = 13\,\mathrm{TeV}$ are used to measure the $\mathrm{t\bar{t}}$ cross section in the $e\mu$ final state [9]. Events are selected based on the

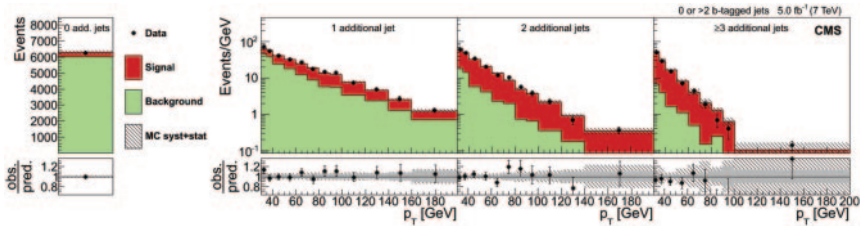

(a)

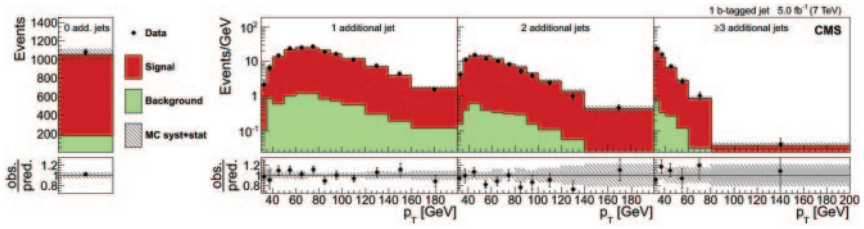

(b)

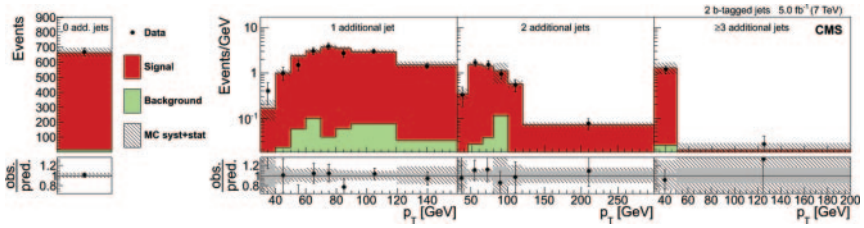

(c)

Fig. 2. – Fitted total event yield for zero additional non-b-tagged jets (left) and p_{T} of the non-b-tagged jet with the lowest p_{T} in the event (right) for events with one, two, and at least three additional non-b-tagged jets, and with zero or more than two (a), one (b), and two (c) b-tagged jets at $\sqrt{s} = 7\,\mathrm{TeV}$ [8]. The last bin of the p_{T} distributions includes the overflow events. The hatched bands correspond to the sum of statistical and systematic uncertainties in the event yield for the sum of signal and background predictions after the fit, and include all correlations. The ratios of data to the sum of the predicted yields are shown at the bottom of each plot. Here, an additional solid gray band represents the contribution from the statistical uncertainty in the MC simulation.

presence of one isolated high p_{T} electron and muon where those with $m_{e\mu} < 20\,\mathrm{GeV}$ are rejected. At least two central high p_{T} jets are required in the event and no b-jet identification is applied. Figure 3 shows the jet multiplicity distribution before the jet requirements together with the $m_{e\mu}$ distribution. The Drell-Yan background is corrected using events containing a same-flavor lepton pair with their $m_{\ell\ell}$ compatible with the Z boson mass. The backgrounds from non-prompt leptons are estimated in a same-sign control data sample. The background contributions are subtracted from the data yield and the result is corrected for the acceptance, signal selection efficiency and the $\mathcal{B}(\mathrm{t\bar{t}} \to \mathrm{b\bar{b}}e\mu)$. Assuming $m_{\mathrm{t}} = 172.5\,\mathrm{GeV}$, the measurement yields $\sigma_{\mathrm{t\bar{t}}}(13\,\mathrm{TeV}) = 746 \pm 58\,(\mathrm{stat.}) \pm 53\,(\mathrm{syst.}) \pm 36\,(\mathrm{lumi.})\,\mathrm{pb}$, in agreement with the SM $\sigma_{\mathrm{t\bar{t}}} = 831^{+40.2}_{-45.6}$. The measured $\sigma_{\mathrm{t\bar{t}}}$ reduces by 0.7% assuming the world average of $m_{\mathrm{t}} = 173.34\,\mathrm{GeV}$ [10].

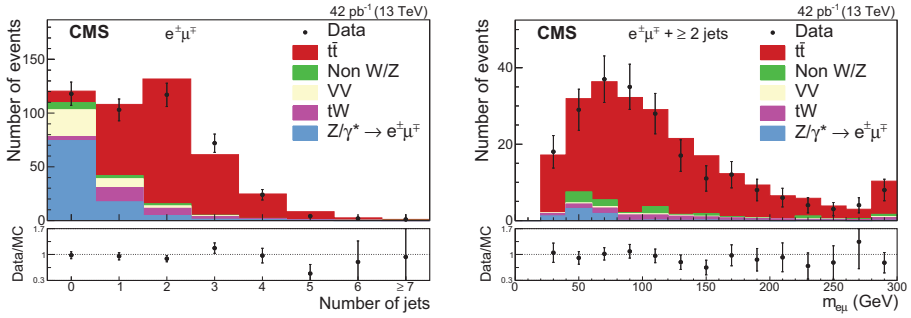

(a) (b)

Fig. 3. – The distributions of (a) the jet multiplicity in events passing the dilepton criteria, and (b) $m_{e\mu}$ after all selection criteria [9]. The expected distributions for $t\bar{t}$ signal and individual backgrounds are shown after implementing data-based corrections; the last bin contains the overflow in events. The ratios of data to the sum of the expected yields are given at the bottom of each panel.

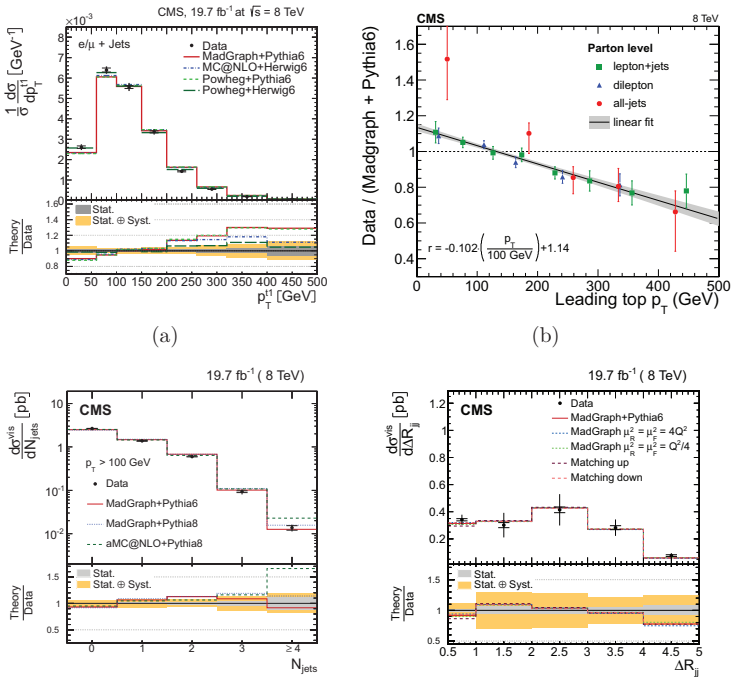

(a) (b)

(c) (d)

Fig. 4. – The differential distribution from CMS Run I measurements: (a) leading top quark p_{T} [11] in $e\mu$ final state, (b) the measured leading top quark p_{T} compared to MadGraph plus Pythia expectations in all final states [12], and in dilepton $t\bar{t}$ events, (c) the multiplicity of additional jets with $p_{\mathrm{T}} > 100\,\mathrm{GeV}$ [13], and (d) the ΔR between the two additional jets with $p_{\mathrm{T}} > 30\,\mathrm{GeV}$ [13].

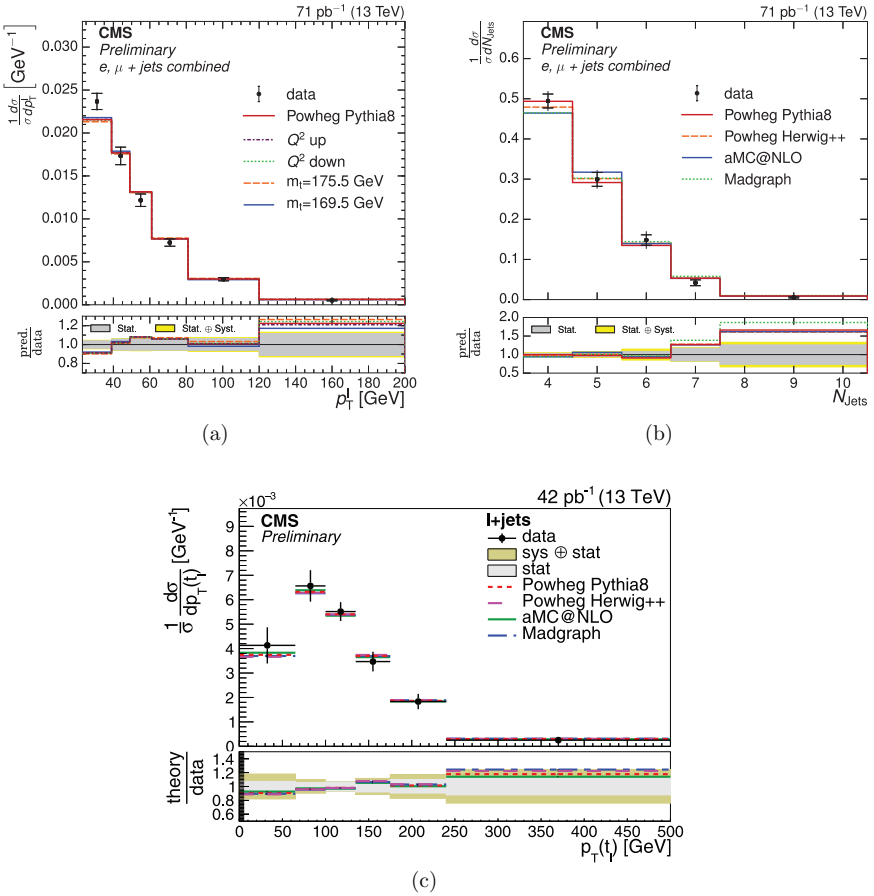

Fig. 5. – The first CMS differential measurements in ℓ+jets events: (a) the lepton p_{T} and (b) the jet multiplicity, compared to particle level objects within the fiducial volume [14], together with (c) the p_{T} of the leptonically decaying top quark, compared to the parton level in the full phase space [15].

4. – Differential $\sigma_{\mathrm{t\bar{t}}}$ measurements

The large top quark data sample in Run I made it possible to study a variety of differential distributions in all $\mathrm{t\bar{t}}$ final states. The distributions range from the kinematics of top quark decay products and additional jets in the event to the properties of the reconstructed top quarks. The MC modeling of $\mathrm{t\bar{t}}$ events are validated through fiducial differential measurements while such measurements in the full phase space, provide valuable inputs to theory calculations. Figure 4(a) shows, in the full phase space, the differential distribution of the p_{T} of the leading reconstructed top quark in the $e\mu$ final state at 8 TeV [11]. In fig. 4(b), the distribution is compared with the outcome of the MadGraph [16, 17] event generator interfaced with Pythia6 [18] for different $\mathrm{t\bar{t}}$ final states where a decreasing trend with $p_{\mathrm{T}}^{\mathrm{top}}$ is observed [12]. The differential $\sigma_{\mathrm{t\bar{t}}}$ in bins of additional jets with $p_{\mathrm{T}} > 100\,\mathrm{GeV}$ within the fiducial volume is shown in fig. 4(c) while the effect of systematic variations of the modeling parameters on the ΔR between

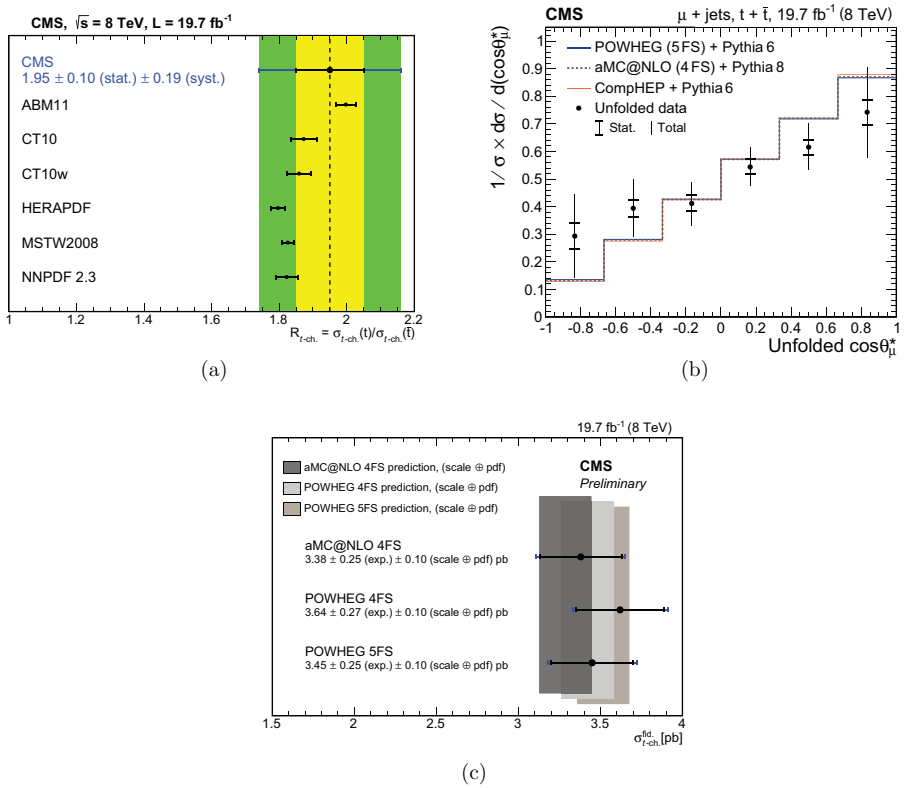

Fig. 6. – Selected CMS t-channel single-top measurements in Run I: (a) comparison of the measured $R_{t\text{-ch.}}$ with predictions by different PDF sets [5], (b) normalized differential $\sigma_{t\text{-ch.}}$ as a function of $\cos\theta_\mu$ [19], and (c) $\sigma^{\text{fid.}}_{t\text{-ch.}}$ measured with different MC generators and compared to the corresponding predictions. The inner error bars represent the experimental uncertainties [20].

the two additional jets ($p_{\text{T}} > 100\,\text{GeV}$) in the full phase space is presented in fig. 4(d). A good data-MC agreement is observed in both cases [13].

The differential measurements in Run II have been exercised using the very first inverse picobarn of the collision data. In the ℓ+jets final state, the distributions of the lepton and jet kinematics as well as the jet multiplicity are examined within the fiducial volume using a data sample with an integrated luminosity of $71\,\text{pb}^{-1}$ [14]. The data are unfolded, after background subtraction, to the particle level in which physics objects at generator level are reconstructed and selected as closely as possible to the detector level. The data and simulations are found to be in a fair agreement (fig. 5(a, b)). The properties of the reconstructed top quark are also studied in a data sample corresponding to an integrated luminosity of $42\,\text{pb}^{-1}$ [15]. The hadronically decaying top quarks are reconstructed using a two-dimensional probability which is based on the compatibility of the di-jet and tri-jet invariant masses with m_{W} and m_{top}, respectively. Events with low probability for the hadronic top quark hypothesis are rejected. On the leptonic side, the sets of kinematic equations for the energy-momentum conservation among the decay products are solved simultaneously, using m_{W} and m_{top} as constraints. The background-subtracted data are unfolded to parton level, *i.e.*, compared with the top quark parton

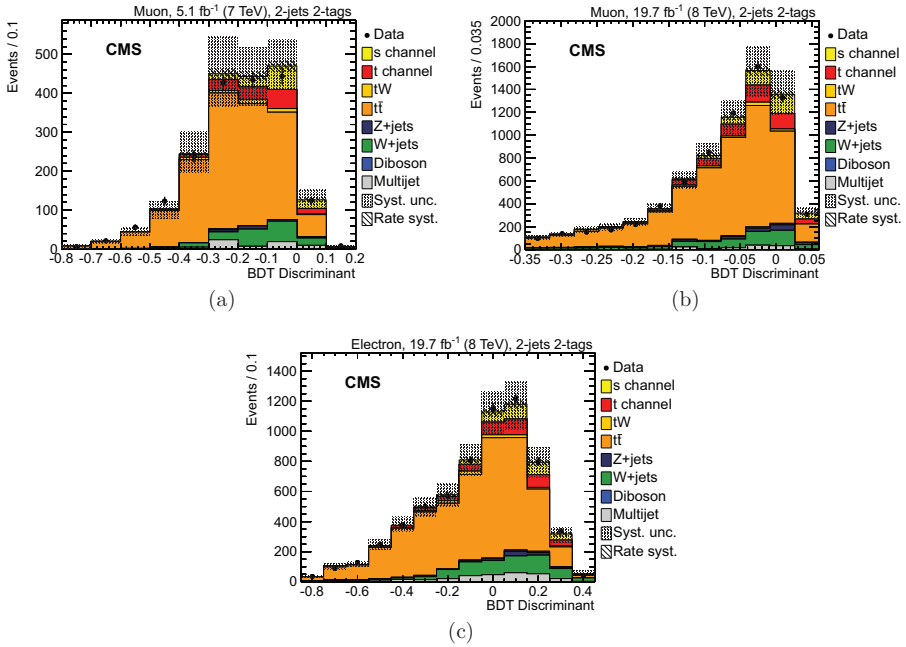

Fig. 7. – The BDT discriminant in the signal region of the s-channel analysis for (a) the muon channel at 7 TeV, (b) muon channel at 8 TeV and (c) the electron channel at 8 TeV [21].

after radiations and before the decay. According to fig. 5(c), a good agreement is observed between the unfolded data and simulation.

5. – Single-top measurements

The t-channel single-top production has been studied in details with the data recorded by CMS during Run I. In addition to the inclusive cross section, the ratio of $R_{t\text{-ch.}} \equiv \frac{\sigma_t}{\sigma_{\bar{t}}}$ that can eventually be sensitive to different PDF choices is measured [5] as shown in fig. 6(a). The top quark spin asymmetry measurement [19], $0.26 \pm 0.03\,(\text{stat.}) \pm 0.10\,(\text{syst.})$, is found to be compatible with the SM prediction of 0.44 within 2σ. The distribution is illustrated in fig. 6(b). Different t-channel modelings are also compared in the fiducial measurement of $\sigma_{t\text{-ch.}}$ [20], as demonstrated in fig. 6(c).

The tW production was first observed by CMS [6] while limits are set on $\sigma_{s\text{-ch.}}$ that is the most abundant production mechanism [21]. The ℓ+jets events were exploited for the latter, where a simultaneous fit to a boosted decision tree discriminant (BDT) is performed in categories with different jets and b-jets multiplicities, allowing to control the W + jets and $\mathrm{t\bar{t}}$ backgrounds. The combined measurement of the signal strength, $\hat{\mu} \equiv \frac{\sigma_{\text{meas.}}}{\sigma_{\text{SM}}}$, in the 7 TeV ($\mu$+jets) and 8 TeV ($\ell$+jets) data samples yields a significance of 2.5σ (1.1σ expected), corresponding to $\hat{\mu} < 4.7$ (3.1 expected) at 95% confidence level (see fig. 7). The dominant systematic uncertainty is found to be the JES. The single-top analyses at 13 TeV started with an early measurement of the t-channel [22] with $42\,\text{pb}^{-1}$ of data which soon updated using the entire 2015 data sample [23]. For the early analysis, events with a muon and two jets are used where one of the jets is identified as b-jet.

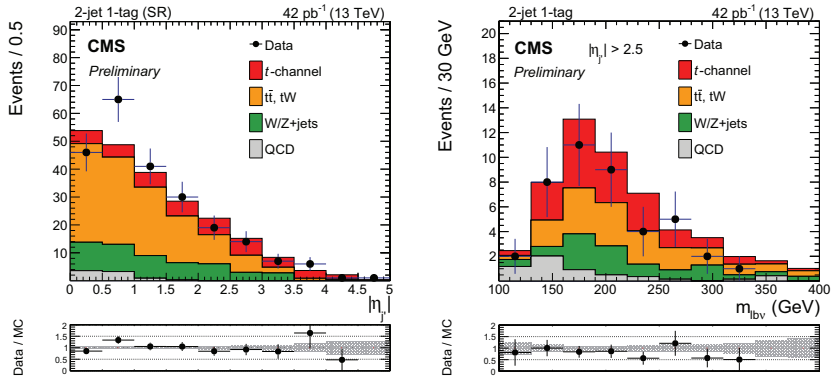

(a) (b)

Fig. 8. – The post-fit distribution of (a) $|\eta_{j'}|$ in the signal region of the t-channel analysis at 13 TeV together with (b) the mass of the top quark candidate in the t-channel enriched region [22].

Events are further required to have $m_{\mu b\nu}$ close to the top quark mass. A simultaneous fit to the pseudorapidity of the non-b-jet, $|\eta_{j'}|$, is performed in the signal region and a region enriched with $t\bar{t}$ backgrounds. The W + jets background is validated in the $m_{\mu b\nu}$ side bands. The measurement yields $\sigma_{t\text{-ch.}}(13\,\text{TeV}) = 274 \pm 98\,(\text{stat.}) \pm 52\,(\text{syst.}) \pm 33\,(\text{lumi.})$ pb, in agreement with the SM prediction, $\sigma_{t\text{-ch.}} = 217 \pm 8.4$. Figure 8 illustrates the distribution of $|\eta_{j'}|$ in the signal region and of the $m_{\mu b\nu}$ in the signal region with large $|\eta_{j'}|$ values.

6. – Summary

The CMS experiment has performed detailed studies of top quark events produced in pair through strong interactions and in single mode vie electroweak processes. The cross

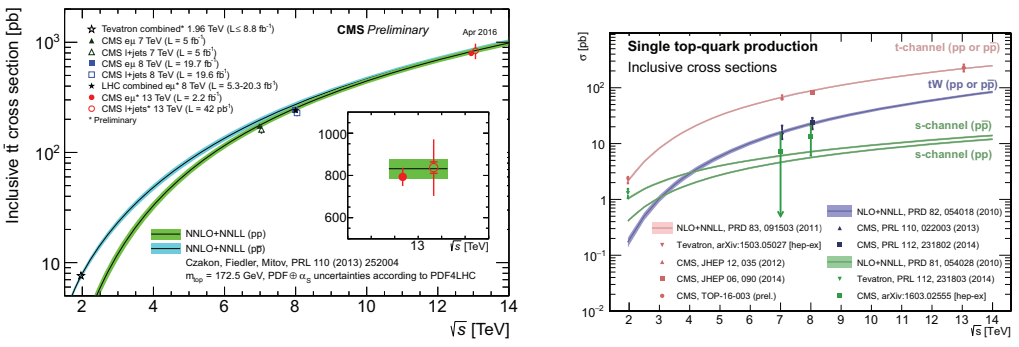

(a) (b)

Fig. 9. – The summary of CMS cross section measurements of $t\bar{t}$ (a) and single-top (b) processes. The t-channel result at 13 TeV [23] with the entire 2015 data supersedes the early analysis described in this article [22].

section measurements are provided inclusively and differentially, within the full phase space and/or the fiducial volume. Some of the early results at 13 TeV have already been updated with the full 2015 data sample. Figure 9 summarizes the results of the inclusive measurements, compared with the theory predictions at different center-of-mass energies.

* * *

The author would like to thank the LHC team and the CMS collaboration at CERN for the excellent work in providing these results. Also thanks to FNRS (Fond National de la Recherche Scientifique) from Belgium who financially supported the author for this conference.

REFERENCES

[1] CDF Collaboration, *Phys. Rev. Lett.*, **74** (1995) 2626.
[2] D0 Collaboration, *Phys. Rev. Lett.*, **74** (1995) 2632.
[3] CMS Collaboration, *JINST*, **3** (2008) S08004.
[4] CMS Collaboration, preprint arXiv:1603.02303 [hep-ex].
[5] CMS Collaboration, *JHEP*, **06** (2014) 090.
[6] CMS Collaboration, *Phys. Rev. Lett.*, **112** (2014) 231802.
[7] CMS Collaboration, preprint arXiv:1602.09024 [hep-ex].
[8] CMS Collaboration, preprint arXiv:1603.02303 [hep-ex].
[9] CMS Collaboration, *Phys. Rev. Lett.*, **116** (2016) 052002.
[10] ATLAS, CDF, CMS and D0 Collaborations, preprint arXiv:1403.4427 [hep-ex].
[11] CMS Collaboration, *Eur. Phys. J. C*, **75** (2015) 542.
[12] CMS Collaboration, *Eur. Phys. J. C*, **76** (2016) 128.
[13] CMS Collaboration, *Eur. Phys. J. C*, **76** (2016) 379, arXiv:1510.03072 [hep-ex].
[14] CMS Collaboration, CMS-PAS-TOP-15-013, `https://cds.cern.ch/record/2064420`.
[15] CMS Collaboration, CMS-PAS-TOP-15-005, `https://cds.cern.ch/record/2048622`.
[16] Alwall J. *et al.*, *JHEP*, **06** (2011) 128.
[17] Alwall J. *et al.*, *JHEP*, **07** (2014) 079.
[18] Sjöstrand, T. *et al.*, *JHEP*, **05** (2006) 026.
[19] CMS Collaboration, *JHEP*, **04** (2016) 073.
[20] CMS Collaboration, CMS-PAS-TOP-15-007, `https://cds.cern.ch/record/2055528`.
[21] CMS Collaboration, preprint arXiv:1603.02555 [hep-ex].
[22] CMS Collaboration, CMS-PAS-TOP-15-004, `https://cds.cern.ch/record/2052187`.
[23] CMS Collaboration, CMS-PAS-TOP-16-003, `https://cds.cern.ch/record/2141577`.